

# Energy consumption in optical modulators for interconnects

David A. B. Miller\*

Ginzton Laboratory, Stanford University, 348 Via Pueblo Mall, Stanford California, 94305-4088, USA  
\*[dabm@ee.stanford.edu](mailto:dabm@ee.stanford.edu)

**Abstract:** We analyze energy consumption in optical modulators operated in depletion and intended for low-power interconnect applications. We include dynamic dissipation from charging modulator capacitance and net energy consumption from absorption and photocurrent, both in reverse and small forward bias. We show that dynamic dissipation can be independent of static bias, though only with specific kinds of bias circuits. We derive simple expressions for the effects of photocurrent on energy consumption, valid in both reverse and small forward bias. Though electroabsorption modulators with large reverse bias have substantial energy penalties from photocurrent dissipation, we argue that modulator diodes with thin depletion regions and operating in small reverse and/or forward bias could have little or no such photocurrent energy penalty, even conceivably being more energy-efficient than an ideal loss-less modulator.

©2012 Optical Society of America

OCIS codes: (250.4110) Modulators; (200.4650) Optical interconnects.

---

## References and links

1. D. A. B. Miller, "Optics for low-energy communication inside digital processors: quantum detectors, sources, and modulators as efficient impedance converters," *Opt. Lett.* **14**(2), 146–148 (1989).
2. D. A. B. Miller, "Physical reasons for optical interconnection," *Int. J. Optoelectron.* **11**, 155–168 (1997).
3. D. A. B. Miller, "Device requirements for optical interconnects to silicon chips," *Proc. IEEE* **97**(7), 1166–1185 (2009).
4. A. V. Krishnamoorthy and D. A. B. Miller, "Scaling optoelectronic-VLSI circuits into the 21st century: A Technology Roadmap," *IEEE J. Sel. Top. Quantum Electron.* **2**(1), 55–76 (1996).
5. K.-H. Koo, P. Kapur, and K. C. Saraswat, "Compact performance models and comparisons for gigascale on-chip global interconnect technologies," *IEEE Trans. Electron. Dev.* **56**(9), 1787–1798 (2009).
6. G. T. Reed, G. Mashonovich, F. Y. Gardes, and D. J. Thomson, "Silicon optical modulators," *Nat. Photonics* **4**(8), 518–526 (2010).
7. Q. Xu, D. Fattal, and R. G. Beausoleil, "Silicon microring resonators with 1.5-microm radius," *Opt. Express* **16**(6), 4309–4315 (2008).
8. F. Y. Gardes, A. Brimont, P. Sanchis, G. Rasigade, D. Marris-Morini, L. O'Faolain, F. Dong, J. M. Fédéli, P. Dumon, L. Vivien, T. F. Krauss, G. T. Reed, and J. Martí, "High-speed modulation of a compact silicon ring resonator based on a reverse-biased pn diode," *Opt. Express* **17**(24), 21986–21991 (2009).
9. P. Dong, S. Liao, D. Feng, H. Liang, D. Zheng, R. Shafiiha, C.-C. Kung, W. Qian, G. Li, X. Zheng, A. V. Krishnamoorthy, and M. Asghari, "Low  $V_{pp}$ , ultralow-energy, compact, high-speed silicon electro-optic modulator," *Opt. Express* **17**(25), 22484–22490 (2009).
10. P. Dong, S. Liao, H. Liang, W. Qian, X. Wang, R. Shafiiha, D. Feng, G. Li, X. Zheng, A. V. Krishnamoorthy, and M. Asghari, "High-speed and compact silicon modulator based on a racetrack resonator with a 1 V drive voltage," *Opt. Lett.* **35**(19), 3246–3248 (2010).
11. G. Li, X. Zheng, J. Yao, H. Thacker, I. Shubin, Y. Luo, K. Raj, J. E. Cunningham, and A. V. Krishnamoorthy, "25Gb/s 1V-driving CMOS ring modulator with integrated thermal tuning," *Opt. Express* **19**(21), 20435–20443 (2011).
12. M. Ziebell, D. Marris-Morini, G. Rasigade, P. Crozat, J.-M. Fédéli, P. Grosse, E. Cassan, and L. Vivien, "Ten Gbit/s ring resonator silicon modulator based on interdigitated PN junctions," *Opt. Express* **19**(15), 14690–14695 (2011).
13. M. R. Watts, W. A. Zortman, D. C. Trotter, R. W. Young, and A. L. Lentine, "Vertical junction silicon microdisk modulators and switches," *Opt. Express* **19**(22), 21989–22003 (2011).
14. J. Liu, M. Beals, A. Pomerene, S. Bernardis, R. Sun, J. Cheng, L. C. Kimerling, and J. Michel, "Waveguide-integrated, ultralow-energy GeSi electro-absorption modulators," *Nat. Photonics* **2**(7), 433–437 (2008).

15. N.-N. Feng, D. Feng, S. Liao, X. Wang, P. Dong, H. Liang, C.-C. Kung, W. Qian, J. Fong, R. Shafiqi, Y. Luo, J. Cunningham, A. V. Krishnamoorthy, and M. Asghari, "30GHz Ge electro-absorption modulator integrated with 3  $\mu\text{m}$  silicon-on-insulator waveguide," *Opt. Express* **19**(8), 7062–7067 (2011).
16. N.-N. Feng, S. Liao, D. Feng, X. Wang, P. Dong, H. Liang, C.-C. Kung, W. Qian, Y. Liu, J. Fong, R. Shafiqi, Y. Luo, J. Cunningham, A. V. Krishnamoorthy, and M. Asghari, "Design and fabrication of 3 $\mu\text{m}$  silicon-on-insulator waveguide integrated Ge electro-absorption modulator," *Opt. Express* **19**(9), 8715–8720 (2011).
17. A. E.-J. Lim, T.-Y. Liow, F. Qing, N. Duan, L. Ding, M. Yu, G.-Q. Lo, and D.-L. Kwong, "Novel evanescent-coupled germanium electro-absorption modulator featuring monolithic integration with germanium p-i-n photodetector," *Opt. Express* **19**(6), 5040–5046 (2011).
18. J. E. Roth, O. Fidaner, R. K. Schaevitz, Y.-H. Kuo, T. I. Kamins, J. S. Harris, and D. A. B. Miller, "Optical modulator on silicon employing germanium quantum wells," *Opt. Express* **15**(9), 5851–5859 (2007).
19. J. E. Roth, O. Fidaner, E. H. Edwards, R. K. Schaevitz, Y.-H. Kuo, N. C. Helman, T. I. Kamins, J. S. Harris, and D. A. B. Miller, "C-band side-entry Ge quantum-well electroabsorption modulator on SOI operating at 1 V swing," *Electron. Lett.* **44**(1), 49–50 (2008).
20. E. H. Edwards, R. M. Audet, S. A. Claussen, R. K. Schaevitz, E. Tasyurek, S. Ren, O. I. Dosunmu, M. S. Ünli, and D. A. B. Miller, "Si-Ge surface-normal asymmetric Fabry-Perot electro-absorption modulator," *CLEO (May 16–21, 2010)*, San Jose, CA, Paper CTuA5.
21. R. M. Audet, E. H. Edwards, P. Wahl, and D. A. B. Miller, "Investigation of limits to the optical performance of asymmetric Fabry-Perot electroabsorption modulators," *IEEE J. Quantum Electron.* **48**(2), 198–209 (2012).
22. R. K. Schaevitz, D. S. Ly-Gagnon, J. E. Roth, E. H. Edwards, and D. A. B. Miller, "Indirect absorption in germanium quantum wells," *AIP Advances* **1**(3), 032164 (2011).
23. R. K. Schaevitz, E. H. Edwards, J. E. Roth, E. T. Fei, Y. Rong, P. Wahl, T. I. Kamins, J. S. Harris, and D. A. B. Miller, "Simple electroabsorption calculator for designing 1310nm and 1550nm modulators using germanium quantum wells," *IEEE J. Quantum Electron.* **48**(2), 187–197 (2012).
24. E. H. Edwards, R. M. Audet, E. Fei, G. Shambat, R. K. Schaevitz, Y. Rong, S. A. Claussen, T. I. Kamins, J. Vuckovic, J. S. Harris, and D. A. B. Miller, "Ge quantum well resonator modulators," 8th Int. Conf. Group IV Photonics, London, Sept. 2011, Paper P1.9.
25. S. Ren, Y. Rong, S. A. Claussen, R. K. Schaevitz, T. I. Kamins, J. S. Harris, and D. A. B. Miller, "Ge/SiGe quantum well waveguide modulator monolithically integrated with SOI waveguides," *IEEE Photon. Technol. Lett.* **24**(6), 461–463 (2012).
26. M. Gould, T. Baehr-Jones, R. Ding, S. Huang, J. Luo, A. K.-Y. Jen, J.-M. Fedeli, M. Fournier, and M. Hochberg, "Silicon-polymer hybrid slot waveguide ring-resonator modulator," *Opt. Express* **19**(5), 3952–3961 (2011).
27. K. Tharmalingam, "Optical absorption in the presence of a uniform field," *Phys. Rev.* **130**(6), 2204–2206 (1963).
28. J. D. Dow and D. Redfield, "Electroabsorption in semiconductors: the excitonic absorption edge," *Phys. Rev. B* **1**(8), 3358–3371 (1970).
29. D. A. B. Miller, D. S. Chemla, and S. Schmitt-Rink, "Relation between electroabsorption in bulk semiconductors and in quantum wells: The quantum-confined Franz-Keldysh effect," *Phys. Rev. B Condens. Matter* **33**(10), 6976–6982 (1986).
30. D. A. B. Miller, D. S. Chemla, T. C. Damen, A. C. Gossard, W. Wiegmann, T. H. Wood, and C. A. Burrus, "Electric field dependence of optical absorption near the bandgap of quantum well structures," *Phys. Rev. B* **32**(2), 1043–1060 (1985).
31. Y.-H. Kuo, Y.-K. Lee, Y. Ge, S. Ren, J. E. Roth, T. I. Kamins, D. A. B. Miller, and J. S. Harris, "Strong quantum-confined Stark effect in germanium quantum-well structures on silicon," *Nature* **437**(7063), 1334–1336 (2005).
32. Y.-H. Kuo, Y. K. Lee, Y. Ge, S. Ren, J. E. Roth, T. I. Kamins, D. A. B. Miller, and J. S. Harris, Jr., "Quantum-confined Stark effect in Ge/SiGe quantum wells on Si for optical modulators," *IEEE J. Sel. Top. Quantum Electron.* **12**(6), 1503–1513 (2006).
33. R. K. Schaevitz, J. E. Roth, S. Ren, O. Fidaner, and D. A. B. Miller, "Material properties in Si-Ge/Ge quantum wells," *IEEE J. Sel. Top. Quantum Electron.* **14**(4), 1082–1089 (2008).
34. D. J. Paul, "Si/SiGe heterostructures: from material and physics to devices and circuits," *Semicond. Sci. Technol.* **19**(10), R75–R108 (2004).
35. K. W. Goossen, G. D. Boyd, J. E. Cunningham, W. Y. Jan, D. A. B. Miller, D. S. Chemla, and R. M. Lum, "GaAs-AlGaAs multiquantum well reflection modulators grown on GaAs and silicon substrates," *IEEE Photon. Technol. Lett.* **1**(10), 304–306 (1989).
36. S. Ren, Y. Rong, T. I. Kamins, J. S. Harris, and D. A. B. Miller, "Selective epitaxial growth of Ge/Si<sub>0.15</sub>Ge<sub>0.85</sub> quantum wells on Si substrate using reduced pressure chemical vapor deposition," *Appl. Phys. Lett.* **98**(15), 151108 (2011).
37. T. N. Theis and P. M. Solomon, "In quest of the 'next switch': prospects for greatly reduced power dissipation in a successor to the silicon field-effect transistor," *Proc. IEEE* **98**(12), 2005–2014 (2010).
38. R. S. Tucker, "Green optical communications-part I: energy limitations in transport," *IEEE J. Sel. Top. Quantum Electron.* **17**(2), 245–260 (2011).
39. A. M. Fox, D. A. B. Miller, G. Livescu, J. E. Cunningham, and W. Y. Jan, "Quantum well carrier sweep out: relation to electroabsorption and exciton saturation," *IEEE J. Quantum Electron.* **27**(10), 2281–2295 (1991).

40. J. A. Cavailles, D. A. B. Miller, J. E. Cunningham, P. Li Kam Wa, and A. Miller, "Simultaneous measurements of electron and hole sweep-out from quantum wells and modeling of photoinduced field screening dynamics," *IEEE J. Quantum Electron.* **28**(10), 2486–2497 (1992).
41. S. A. Claussen, E. Tasyurek, J. E. Roth, and D. A. B. Miller, "Measurement and modeling of ultrafast carrier dynamics and transport in germanium/silicon-germanium quantum wells," *Opt. Express* **18**(25), 25596–25607 (2010).
42. T. K. Woodward, W. H. Knox, B. Tell, A. Vinattieri, and M. T. Asom, "Experimental studies of proton-implanted GaAs-AlGaAs multiple-quantum-well modulators for low-photocurrent applications," *IEEE J. Quantum Electron.* **30**(12), 2854–2865 (1994).
43. S. Palermo, A. Emami-Neyestanak, and M. Horowitz, "A 90 nm CMOS 16 Gb/s transceiver for optical interconnects," *IEEE J. Solid-state Circuits* **43**(5), 1235–1246 (2008).
44. M. N. Islam, R. L. Hillman, D. A. B. Miller, D. S. Chemla, A. C. Gossard, and J. H. English, "Electroabsorption in GaAs/AlGaAs coupled quantum well waveguides," *Appl. Phys. Lett.* **50**(16), 1098–1100 (1987).
45. K. W. Goossen, J. E. Cunningham, D. A. B. Miller, W. Y. Jan, A. L. Lentine, A. M. Fox, and N. K. Ailawadi, "Low field electroabsorption and self-biased self-electrooptic effect device using slightly asymmetric coupled quantum wells," Paper MB3, Topical Meeting on Quantum Optoelectronics, Salt Lake City, March 1991 (Optical Society of America, 1991).
46. J. S. Weiner, A. C. Gossard, J. H. English, D. A. B. Miller, D. S. Chemla, and C. A. Burrus, "Low voltage modulator and self-biased self-electro-optic effect device," *Electron. Lett.* **23**(2), 75–77 (1987).

## 1. Introduction

Because of the quantum nature of optical detection [1], optics could reduce the energy for transmitting information even at short distances inside computers and information switching and processing machines [1–3]. Electrical interconnects in practice have to charge the capacitances in electrical lines to the signal voltage. Optics avoids that electrostatic energy, requiring only the energy to drive the optical transmitter devices (e.g., lasers or modulators) and run any receiver amplifiers [3–5].

Especially for short distances, such as connections to or even within electronic chips, the energy targets for optical transmitter devices are aggressive – possibly ~100 fJ/bit for longer off-chip distances, 10's of fJ/bit for dense off-chip connections and a few fJ/bit for global on-chip connections [3]. Modulators are particularly attractive for low energy transmitters because, unlike lasers, they do not have a threshold that could limit the minimum operating energy, and they may be easier to integrate monolithically with silicon.

There are various modulator approaches for integration with silicon [6]. Examples include the predominantly electro-refractive carrier injection, carrier accumulation, and carrier depletion devices using silicon as the active medium – especially low-energy, high-speed silicon ring [7–12] or disk resonators [13], electroabsorptive devices using GeSi [14], Ge [15–17], or Ge quantum wells [18–25] on silicon, and rings with electro-optic polymers [26]. Carrier depletion and electroabsorptive devices typically utilize diode structures in reverse or small forward bias. Such biasing conditions avoid dissipation from forward currents and speed limits from carrier recombination times and can enable high-speed low-energy operation.

The physical mechanisms of electroabsorption (Franz-Keldysh Effect (FKE) [27, 28] and, especially, the related [29] Quantum-Confined Stark Effect (QCSE) in quantum wells [30–33]) are particularly strong, allowing relatively low energies even without resonators. By contrast, low-energy Si modulators typically require precisely-tuned high-Q resonators (e.g.,  $Q \sim 10,000$ ). As we clarify below, for example, one recent such QCSE device [25] without such resonators has a dynamic dissipation of ~0.75fJ, lower than any reported Si device.

Ge-based modulator devices are promising for integration with silicon-based electronics, where Ge is already used extensively [34]. Modulators, unlike lasers, also appear to be relatively tolerant of the crystal defects that arise under lattice-mismatched epitaxial growth [35], with even III-V's on Si successfully demonstrated [35].

In this paper, we analyze energy in depletion-based modulator devices so that we might better predict overall energy performance, design devices and drive circuits for minimum energy, and provide a fair comparison between approaches. Our analysis suggests promising directions especially for electroabsorptive devices, such as low or even forward biasing.

Various mechanisms contribute to energy consumption in reverse- or slightly forward-biased diode devices, including, (i) charging and discharging of the device capacitance (dynamic dissipation), and, in electroabsorptive devices, the “static” dissipations from (ii) absorption of optical power and (iii) dissipation from photocurrent flow. In quantum-well electroabsorption modulators in particular static biasing can increase the sensitivity to small additional voltage changes. Additionally, because the absorption edge can remain quite abrupt even with large bias [23, 36], such bias allows the modulator’s operating wavelength to be voltage-tuned while still allowing low drive swing [19, 23, 36]. Such static bias can, however, lead to additional dissipation from photocurrent and to some consequences for the dynamic dissipation of the modulator that we discuss below. Silicon resonator modulators [6, 13] can also require significant powers and energies per bit for tuning, though we will not discuss this here.

We presume the modulators can be modeled as a fixed capacitor with a parallel current source from any photocurrent. For the  $p-i-n$  diodes typically used in electroabsorption devices, the thickness of the  $i$ -region largely determines the capacitance, with only small voltage dependence of capacitance from depletion into the  $p$  and  $n$  regions. Fixed capacitance is a substantial approximation for some silicon carrier depletion modulators that may not use  $p-i-n$  diodes, but our model should allow reasonable comparisons. This model also covers electrorefractive (electro-optic) devices in the form of either biased insulating materials, such as electro-optic polymers [26], or diodes; presumably these would have little if any photocurrent.

We start by analyzing the dynamic dissipation associated with charging and discharging the capacitance, and continue with the static dissipation from absorption and photocurrent. Finally, after summarizing dissipation results, we discuss implications for device design.

## 2. Dissipation from capacitive charging and discharging

In charging and discharging a capacitor, the unavoidable dissipation is associated with the current flowing through the series resistance in the circuit. Here, we consider all the series resistances (including those of any driver circuit and of the modulator contacts) to be gathered into one effective series resistance  $R$ . This gathering together makes no difference to the final energy consumption in our approach. As will be clarified in Section 2.2, the resistor may also be nonlinear (i.e., depending on voltage) without changing our energy results, so this lumped resistance also models the transistor output characteristics as far as those matter here.

### 2.1 Model drive circuit

To analyze energy consumption properly, we need to consider the circuit that charges and discharges the modulator capacitance  $C$ , at least in a simplified form. Figure 1(a) shows an example circuit based on a CMOS inverter, which swings its output between 0 V and  $V_{DD}$ . An additional (reverse) bias of magnitude  $V_B$  is also applied to the modulator. Figure 1(b) shows an equivalent circuit where we have replaced the output stage with a switch, which can be toggled between 0V and  $V_{DD}$ , together with our lumped series resistor  $R$ . The total charge flowing through the modulator is represented by the current source  $I_R$ , which could include both photocurrent and leakage current. For simplicity we neglect leakage here, though it could easily be added if needed. In Fig. 1, we also show an optional bypass capacitor  $C_{BP}$ , whose important function we explain later. For static dissipations, we neglect any voltage drop  $I_R R$  across the resistor  $R$  from the current flow  $I_R$ , presuming sufficiently small resistances.

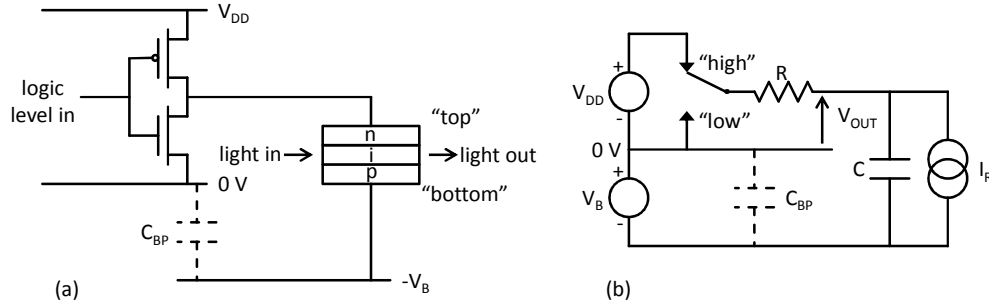


Fig. 1. (a) Example drive circuit for a  $p$ - $i$ - $n$  modulator diode. (b) Equivalent circuit.

## 2.2 Dynamic energy calculation

Suppose then we change the switch from “low” to “high”. The voltage across  $C$  will change from  $V_B$  to  $V_B + V_{DD}$ . Because the electrostatic stored energy in a capacitor  $C$  at a voltage  $V$  is  $(1/2)CV^2$ , the change in energy in the capacitor is

$$\Delta E_{CES} = (1/2)C \left[ (V_B + V_{DD})^2 - V_B^2 \right] = (1/2)CV_{DD}^2 + CV_{DD}V_B \quad (1)$$

Note here that the total energy involved in changing the voltage across the capacitor by an amount  $V_{DD}$  is not simply  $(1/2)CV_{DD}^2$ .

The charge  $Q$  required to change the voltage on the capacitor  $C$  by  $V_{DD}$  is  $Q = CV_{DD}$ . This charge has been supplied by the  $V_{DD}$  voltage source at a voltage  $V_{DD}$ , so that voltage supply has provided an energy  $\Delta E_{VDD} = QV_{DD} = CV_{DD}^2$ . The total charge  $Q = CV_{DD}$  also has to flow through the bias voltage supply onto the bottom plate of the capacitor  $C$ . This charge flows at a voltage  $V_B$ , and so there is an energy from the bias supply  $\Delta E_B = QV_B = CV_{DD}V_B$ , which we recognize as the last term on the right in Eq. (1).

The energy dissipated in flowing a charge  $\delta Q$  through a resistor at a voltage  $V$  is  $\delta E = V\delta Q$ . When flowing a charge  $\delta Q$  onto a capacitor  $C$ , the resulting change in voltage  $\delta V$  on the capacitor is such that  $\delta Q = C\delta V$ . In the circuit, the voltage  $V$  across the resistor  $R$  is  $V = V_{DD} - V_{OUT}$ . Hence we find the standard result that the total energy dissipated in the resistor in charging the capacitor  $C$  from 0V to  $V_{DD}$  is

$$\Delta E_R = C \int_0^{V_{DD}} (V_{DD} - V_{OUT}) dV_{OUT} = (1/2)CV_{DD}^2 \quad (2)$$

Note that this energy is independent of the value of the resistance  $R$ , and does not require any particular relation between current and voltage for that resistor; the resistor may be nonlinear.

In summary, in charging the capacitor from a “top” voltage of 0V to  $V_{DD}$  while holding the bottom at a bias voltage of  $-V_B$ , the  $V_{DD}$  supply provides energy  $\Delta E_{VDD} = CV_{DD}^2$ , half of which is provided to the capacitor, and half of which is dissipated in the series resistance, and the  $V_B$  (bias) supply provides an energy  $\Delta E_B = CV_{DD}V_B$  to the capacitor to give the total energy change in the capacitor as in by Eq. (1). Connecting the switch subsequently to 0V discharges the capacitor, leading to a further dissipation  $\Delta E_R = (1/2)CV_{DD}^2$  in the resistor.

This argument leads to a question: what happens to the energy  $\Delta E_B = CV_{DD}V_B$  when we pass the charge  $Q$  back through the bias voltage supply? Is that energy also dissipated? In

other words, is the total energy dissipated per complete charge/discharge cycle just the energy dissipated in the resistor  $R$ , that is

$$\Delta E_{DISS} = 2\Delta E_R = CV_{DD}^2 \quad (3)$$

or does it also include the energy supplied by the bias supply, i.e., a total of  $\Delta E_{DISSB} = 2\Delta E_R + CV_{DD}V_B$ ? The answer depends on the physical nature of the bias voltage source. If we regard the bias voltage as a non-rechargeable battery, the energy cannot usefully be put back into the battery for future use, and will be dissipated in a variety of chemical processes in the battery, generating heat; the energy dissipated per cycle is then  $\Delta E_{DISSB}$ .

There is, however, a simple way to make the bias supply energy  $\Delta E_B = CV_{DD}V_B$  essentially completely recoverable, which is to use a large bypass capacitor  $C_{BP}$  across the bias supply, possibly formally decoupled from the actual bias supply by a series resistor and/or inductor (not shown). Such bypass is commonplace for reducing the effective source impedance of power supplies, though the use for the bias energy recovery discussed here may be less obvious. Assuming the capacitance  $C_{BP}$  is sufficiently large that the voltage across it would not change appreciably during a charge/discharge cycle, this capacitor can be charged and discharged without additional loss, functioning as a perfectly rechargeable battery; all the resistive loss is already accounted for in the loss in the lumped series resistance  $R$ . Hence, with the use of a bypass capacitor, the energy dissipated per complete charge/discharge cycle is as given in Eq. (3). Such capacitance may already be present in the circuit in supply line capacitance. Alternatively, even without a bypass capacitor this charge flow might simply act to reduce the overall current flowing out of the bias supply for other dissipative reasons (e.g., for photocurrent), reducing overall dissipation by  $\Delta E_B$  and achieving the same end result of effectively recovering this energy  $\Delta E_B$ .

In driving a modulator with a real digital signal, the number of charge/discharge cycles depends on the pattern of bits. When sending actual digital data, it is reasonable to expect equal numbers of “ones” and “zeros”. In non-return-to-zero (NRZ) signaling, in which we have changes in the modulator state (i.e., charge or discharge) only when the digital signal changes, there are four possible sequences of bits, all of which would be presumably equally likely - 0-0, 0-1, 1-1, 1-0 [13]. In two of these sequences (0-0 and 1-1) there is no change of state, so no energy is dissipated in charging the capacitor. In the other two (0-1 and 1-0), half of a charge/discharge cycle is involved in each such transition. On the average, therefore, in an effectively random sequence of bits, there is one complete charge/discharge cycle every 4 bits. So, the total dissipated energy per bit would be  $(1/4)\Delta E_{DISS}$  (when using a bypass capacitor over the bias supply) [13, 15], i.e., the dynamic energy per bit becomes

$$\Delta E_{bit} = (1/4)CV_{DD}^2 \quad (4)$$

This relation has been used by recent authors [13, 15]. We have shown here that this number remains valid even in the presence of d.c. bias on the modulator, provided a bypass capacitor is used on the bias supply. We have also given our result in terms of  $V_{DD}$ , the supply voltage, rather than just a peak-to-peak drive voltage,  $V_{pp}$ . If  $V_{pp} \neq V_{DD}$ , then we can expect additional energy dissipated in the resistances in the driver circuit.

**Table 1.**

Modulator type	C	Drive $V_{DD}$	Mod. Depth	Bias $V_B$	$\frac{1}{4}CV_{DD}^2$	Launch Eff. $\beta$	Energy Mag. $1/\beta$
Si disk [13]	12fF	1V	3.2dB	–	3fJ	20–26%	3.8–4.9
GeSi FKE [14]	11fF	3V	8dB	4V	25fJ	4%	25
Ge FKE [15]	25fF	4V	7.5dB	0V	100fJ	6.3%	16
Ge QCSE [25]	3fF	1V	3dB	4V	0.75fJ	5.6%	18
Proposed Ge QCSE design [23]	24fF	1V	5dB	0V	6fJ	17%	6

Table 1 summarizes dynamic dissipations  $(1/4)CV_{DD}^2$  for various published low energy modulators or modulator designs on silicon substrates using silicon [13] and/or germanium [14, 15, 23, 25], materials. Voltages and capacitances come directly from the respective papers, except the capacitance of the silicon disk modulator [13] is inferred from the switching energy. (The other quoted factors  $\beta$  and  $1/\beta$  arise from optical absorption and photocurrent, as discussed in Section 3.) For comparison also, a recent electro-optic polymer ring modulator [26] in silicon slot guides has an estimated capacitance of  $\sim 27$  fF, which, at a drive voltage of 3V swing would have a comparable  $(1/4)CV_{DD}^2$  energy of  $\sim 60$  fJ/bit.

### 2.3 Adiabatic operation

The concept of charging and discharging a capacitor without substantial loss in a non-repetitive signal has been discussed extensively in considering adiabatic electronics (e.g., Ref [37]). If the  $V_{DD}$  supply itself is cycled, for example by repetitively ramping up to a maximum and then ramping down again, then a capacitor can be charged by connecting it to the supply on the up-swing of the voltage and can be discharged by connecting it on the down-swing. Provided the ramp cycle is long compared to the  $RC$  time of the capacitor and its series resistance, essentially arbitrarily small energy need be dissipated to charge or discharge the capacitor (e.g.,  $\Delta E_{AD} = (1/2)CV_{DD}^2 (RC/t_s)$  [37] for a voltage supply ramped linearly from 0V to  $V_{DD}$  over a time  $t_s$ ; this energy can be arbitrarily small if  $t_s \gg RC$ . Whether such approaches will be used commercially is still an open question, in part because they may require low clock rates, but they could largely eliminate dynamic dissipation.

### 3. Energy dissipation from photocurrent

Electroabsorptive devices necessarily absorb some fraction of the input power since that is how they modulate the signal. This absorption leads to additional mechanisms for energy consumption. We seem to have two separate kinds of mechanisms – (i) directly absorbed power from the incident light beam, and (ii) additional power dissipation from photocurrent  $I_{PC}$  flowing over a biased region. We expect that, with some large reverse bias voltage  $V_{TOT}$ , there will be a dissipated power  $\sim I_{PC}V_{TOT}$ ; this is generally true, as we verify below, and it has been included in previous analyses [4, 38]. Here, however, we need a more detailed discussion when considering devices run with low or forward bias voltages, for two reasons: (a) some of the dissipation of the directly absorbed optical power also involves the movement of charge and (b) some of the absorbed power may be recoverable in diode structures because

they can behave as photovoltaic cells. To understand all the energy dissipations, we need to look separately at reverse and forward bias.

### 3.1 Reverse bias dissipation

Most electroabsorption modulators use diode structures, with the active material being in a nominally undoped or intrinsic *i*-region between *p*-doped and *n*-doped contact regions. Such a structure allows the necessary high electric fields (typically up to  $\sim 10^5$  V/cm) to be applied under reverse bias without substantial static current flow (in the absence of photocurrent).

Under reverse bias, it is also common for all or nearly all of the absorbed energy to generate photocurrent, at one electron-hole pair per photon absorbed in the intrinsic region. Photons absorbed in the contact regions may also lead to photocurrent, with carriers diffusing into the *i*-region, but we neglect such absorption here. In QCSE modulators, the contact regions are typically of larger bandgap so that they do not absorb the signal photons anyway.

The reason for the high photocurrent collection efficiency in reverse bias is that the field typically sweeps the carriers out of the *i*-region in a short time, e.g., picoseconds to tens of picoseconds, much shorter than typical recombination times of nanoseconds or longer. Even in quantum well structures, where the barriers can hold the carriers within the wells, the carrier emission (by thermionic and/or tunneling) is typically also on picosecond to 100's of picosecond time-scales [39–41]. Consequently, photocurrent collection often saturates near 100% at low biases (e.g., 1 – 2V or less) as the *i*-region is depleted. It is possible to suppress the photocurrent, for example by ion implantation [42], and hence also the dissipation associated with it, though such approaches can compromise the electroabsorption [42].

We consider first the case of an unbiased homojunction photodiode (Fig. 2(a)), showing the band structure in real space for a homojunction with bandgap energy  $E_G$ . We make the simplifying approximation that the Fermi levels in the *p* and *n* regions are at the valence and conduction band edges. We assume for the moment that the photon energy  $\hbar\omega = E_G$ , which is the case for most electroabsorptive mechanisms since the changes in absorption all occur near to the bandgap energy. In Fig. 2(a), we show a photon being absorbed, generating an electron in the conduction band and a hole in the valence band.

If we hold the overall voltage across the device at zero volts (so that the Fermi levels remain the same at both sides of the device), then the electron will move downhill to the right into the *n*-region, dissipating energy as it does so, for example through electron-phonon scattering, and ending up with an energy approximately equal to the Fermi energy  $E_F$  in the *n*-region. Similarly, the hole will move uphill into the *p*-region on the left, dissipating energy through scattering until it also ends up with energy  $E_F$ . The net result is that a total energy of  $\hbar\omega$  is dissipated, all by scattering of the charge carriers within the diode, generating heat in the diode. One electron of current flows through the external circuit also, but this current flows at zero voltage in this example case, so no energy is dissipated in or sourced from the external electrical circuit. The energy dissipated here has all come from the energy in the photon to start with, so it also corresponds to the absorbed optical energy within the diode.

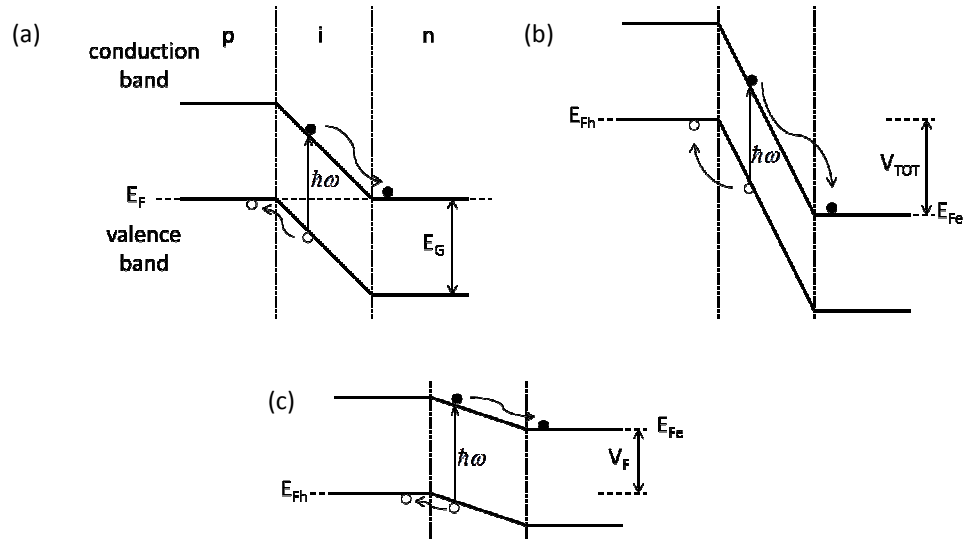


Fig. 2. Diode band diagrams at (a) zero bias; (b) reverse bias  $V_{TOT}$ ; (c) forward bias  $V_F$ .

If we now reverse bias the diode by a voltage of magnitude  $V_{TOT}$ , as in Fig. 2(b), the electron (hole) scatters downhill (uphill) to the  $n$ -region ( $p$ -region) until it ends up at the electron (hole) quasi-Fermi-level  $E_{Fe}$  ( $E_{Fh}$ ), dissipating a total energy  $\delta E_{diss}$  for the electron-hole pair of  $\hbar\omega$  (the absorbed optical energy) plus  $eV_{TOT}$ , i.e.,

$$\delta E_{diss} = \hbar\omega + eV_{TOT} \quad (5)$$

where  $e$  is the magnitude of the electron charge. The flow of an electron of charge through the external circuit requires the power supplies to contribute the energy  $eV_{TOT}$  that is dissipated inside the diode by electron and hole scattering.

### 3.2 Forward bias dissipation

We could run a diode modulator into moderate forward bias  $V_F$  (Fig. 2(c)) provided that  $V_F$  is “small” – that is, sufficiently low that there is negligible forward current flow. We could choose  $V_B$  to be a forward bias of magnitude  $V_F$  ( $= -V_B$ ). The diode would then be reverse biased by an amount  $V_{DD} - V_F$  in the “high” state (when the “top” of the modulator is connected to  $V_{DD}$ ) and forward biased by an amount  $V_F$  in the “low” state (when the “top” of the modulator is connected to 0V). When forward biased, the electron and hole would dissipate an energy  $\hbar\omega - eV_F$  within the diode as they move to their respective contacts, and an energy  $eV_F$  would be put back into the bias supply – a photovoltaic power generation. Presuming the bias supply is reversible (e.g., by bypass capacitance), this energy can be recovered. Hence, per photon, the dissipated energy from photocurrent when the device is under a (small) forward bias of magnitude  $V_F$  is  $\hbar\omega - eV_F$ , which gives us exactly the same expression as Eq. (5) if we understand  $V_{TOT} = -V_F$ , i.e., the “reverse” bias voltage is now negative as required to represent a forward bias.

### 3.2 Indirect gap semiconductors

In the case of a homojunction made from an indirect bandgap material like Ge, the electrical band gap energy is the indirect band gap and the optical absorption of interest takes place near

the higher direct band gap energy, as sketched in Fig. 3(a) for the zero bias case. The answers above (i.e., Eq. (5)) remain unchanged. The photogenerated electron merely scatters down into the lower indirect conduction band edge, a process that likely takes a short time (e.g., < 200 fs [41]). Still the entire photon energy is dissipated in the diode (or partly in the circuit in the forward biased case).

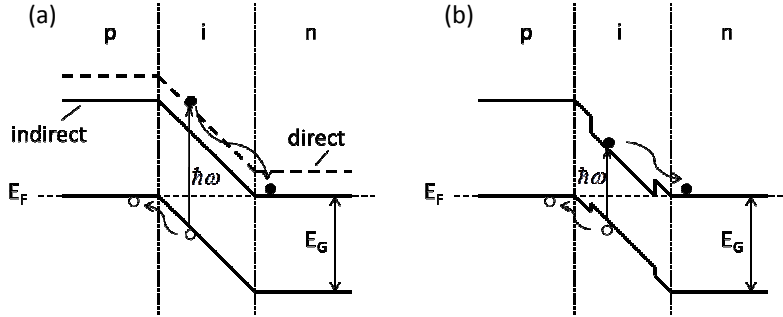


Fig. 3. Diode band structures for (a) indirect gap materials and (b) heterostructures.

### 3.3 Heterojunction diodes

Figure 3(b) shows a heterostructure for the zero bias case with band offsets in the conduction and valence bands between the larger band gap  $p$  and  $n$  regions and a lower band gap material within the  $i$ -region. Here we show the case where the  $i$ -region starts sufficiently within the larger gap material that there is no charge accumulation in the narrower gap material. If the  $i$ -region starts immediately with the narrower gap material, the bands may kink near the heterointerfaces, with the possible formation of charge accumulation layers just inside the  $i$ -region. Still, in either case the electron will move downhill into the  $n$ -region ending up near the electron Fermi level there and similarly for the hole falling up into the  $p$ -region. The precise process by which the electron and hole cross through any “kink” regions will vary with the detailed designs and doping densities but the ultimate result will be the same; still the entire photon energy is dissipated in the diode (or partly in the circuit in the forward biased case). A quantum well structure has essentially the same behaviors as the simple heterostructure of Fig. 3(b). Whether charge accumulation occurs in the quantum wells nearest to the doped contacts or in the “barrier” materials just beside the doped contacts depends on the detailed design of the structure, but still the entire photon energy is dissipated.

### 3.4 Expression for energy dissipation

In all these cases of different structures, the magnitude of the total photocharge generated (of electrons or holes) is  $Q_{PC} = eE_{abs}(V_{TOT})/\hbar\omega$ , where  $E_{abs}(V_{TOT})$  is the absorbed optical energy during some particular bit period for modulator under a total bias voltage  $V_{TOT}$ , and the additional energy associated with flowing  $Q_{PC}$  over a voltage  $V_{TOT}$  is  $Q_{PC}V_{TOT}$ .

Hence regardless of whether we are in reverse or small forward bias, or whether we have a homojunction, a heterojunction, or a quantum well structure, we can use the same expression for the energy dissipation. Specifically, the total energy  $E_{PCA}$  dissipated from photocurrent flow and from net absorption of optical energy in the device when the device is under a total bias voltage  $V_{TOT}$  is given by

$$E_{PCA}(V_{TOT}) = E_{abs}(V_{TOT}) + V_{TOT}Q_{PC} = E_{abs}(V_{TOT}) \left[ 1 + V_{TOT}/(\hbar\omega/e) \right] \quad (6)$$

where we are assuming perfect photocurrent collection efficiency, our convention is that a positive  $V_{TOT}$  corresponds to a reverse bias and  $\hbar\omega/e$  is a voltage numerically equal to the

photon energy in electron-volts. Unlike the dynamic capacitive energy case, adiabatic techniques cannot eliminate this energy because it is dissipated by scattering as the charge carriers move inside the device itself.

### 3.5 Energy per bit from absorption and photocurrent dissipation

To understand the energy per bit, first we have to define some terms. In the conceptually simplest optical communications transmitter we would turn on a light source of power  $P$  for a bit time  $t_{bit}$  to send a “one” and turn it off to send no power for time  $t_{bit}$  to send a “zero”. In a bit stream with equal numbers of “ones” and “zeros”, the average launched energy per bit would then be  $E_{bit\,trans} = Pt_{bit} / 2$ , and the average launched power would be  $P / 2$ . For a hypothetical perfectly efficient light source, on the average the total energy  $E_{bit\,tot}$  required to launch such an energy per bit would also be  $Pt_{bit} / 2$  since all the energy goes into the emitted light. Defining an energy launching efficiency  $\beta$  as

$$\beta = E_{bit\,trans} / E_{bit\,tot} \quad (7)$$

for this ideal transmitter,  $\beta = 1$ . Knowing this efficiency, then the total energy  $E_{bit\,tot}$  we need to supply per bit to launch an average energy per bit of  $E_{bit\,trans}$  is  $E_{bit\,tot} = E_{bit\,trans} / \beta$ .

In a modulator-based transmitter, the output light may not turn off completely, so we consider the useful launched power or energy to be the difference between the power  $P_1$  or energy  $E_1$  launched for a “one” and the power  $P_0$  or energy  $E_0$  launched for a “zero”. To an a.c. coupled receiver, this difference in powers or energies between “one” and a “zero” signals is what matters. Some other receiver designs intended for interconnects, such as the integrating double-sampling design [43], similarly work from this difference. Specifically, then, for the useful launched energy per bit we would have the average

$$E_{bit\,trans} = |E_1 - E_0| / 2 \quad (8)$$

We presume that, after accounting for any coupling losses into the modulator and for any other losses in the modulator other than the optical absorption that takes place within it (e.g., optical scattering losses), there is an optical input energy per bit period of  $E_{ino}$ , which can be transmitted, absorbed, reflected, deflected, or some combination of the these.

For some ideal modulator in a simple “on”/“off” signaling (as in non-return-to-zero (NRZ) signaling), we can imagine that all of the incident optical energy per bit  $E_{ino}$  is transmitted in the “one” state and none in the “zero” state (so  $E_{bit\,trans} = E_{ino} / 2$ ). Now,  $E_{ino}$  would be present at the modulator optical input in every bit period. Hence, even if the only energy involved was the incident optical energy, the launching efficiency for such an ideal modulator would be  $\beta = 0.5$ .

Now, for a real modulator, we can usefully define the optical (power or energy) absorption of the modulator as a function of bias voltage as  $\eta(V_{TOT})$ ; equivalently, this is the fraction of the input energy  $E_{ino}$  that is not transmitted by the modulator. (For example, for a modulator that can be described by an effective absorption coefficient  $\alpha$  over a length  $L$ , we would have  $\eta(V_{TOT}) = 1 - \exp[-\alpha(V_{TOT})L]$ ). For a given voltage bias  $V_{TOT}$  on the modulator, the transmitted optical energy is

$$E_{outo}(V_{TOT}) = [1 - \eta(V_{TOT})] E_{ino} \quad (9)$$

and the absorbed energy  $E_{abs}(V_{TOT})$  is

$$E_{abs}(V_{TOT}) = \eta(V_{TOT})E_{ino} \quad (10)$$

Whether a logic “one” corresponds to a “high” voltage on the modulator or a “low” one depends on the details of the modulator. Typically for a FKE modulator or a QCSE modulator with simple “rectangular” wells, we choose to operate with photon energies below the band gap energy, in which case the absorption typically increases with increasing voltage. We can call such a modulator “normally on” because at low reverse bias voltage it is in its more transmitting state. Quantum well modulators can also be operated at somewhat shorter wavelengths (larger photon energies), especially with coupled well designs, in which case potentially useful modulation can be obtained in which the absorption decreases with increasing (reverse bias) voltage [44,45]. We can call such a modulator “normally off” (it is in its low transmission state at low reverse bias). The use of the modulus in Eq. (8) allows for both possibilities, however. Using Eqs. (9) and (10) we have

$$E_{bit\ trans} = (1/2) \left| E_{outo}(V_{DD} + V_B) - E_{outo}(V_B) \right| = E_{ino} \left| \eta_{hi} - \eta_{lo} \right| / 2 \quad (11)$$

where  $\eta_{hi} = \eta(V_{DD} + V_B)$  and  $\eta_{lo} = \eta(V_B)$ .

The total energy put into the modulator in a given bit period is the sum of the optical input energy,  $E_{ino}$ , and the energy dissipated from photocurrent. The energy  $E_{PCA}(V_{TOT})$  already includes both the photocurrent dissipation energy and any absorbed optical energy, so to get the total energy put into the modulator in a bit period, we only have to add the optical energy that is not absorbed, which is the transmitted energy  $E_{outo}(V_{TOT})$ ; the total energy put into the modulator in a given bit period is therefore  $E_{PCA}(V_{TOT}) + E_{outo}(V_{TOT})$ . Adding up the total energy put into the modulator in each of the two bias conditions and dividing by 2 to get the average, we have the average energy to launch a bit when the optical input energy is  $E_{oin}$ :

$$E_{bit\ tot} = (1/2) \left\{ \left[ E_{PCA}(V_{DD} + V_B) + E_{outo}(V_{DD} + V_B) \right] + \left[ E_{PCA}(V_B) + E_{outo}(V_B) \right] \right\} \quad (12)$$

Substituting from Eqs. (6), (9) and (10) gives, after some algebra,

$$E_{bit\ tot} = E_{ino} \left[ 2 + \eta_{hi}\mu_{hi} + \eta_{lo}\mu_{lo} \right] / 2 \quad (13)$$

Here we have defined convenient “photocurrent dissipation multipliers”  $\mu_{hi} = (V_{DD} + V_B) / (\hbar\omega / e)$  and  $\mu_{lo} = V_B / (\hbar\omega / e)$ , dimensionless numbers that correspond to the respective “high” and “low” total voltages across the diode, expressed in voltage units of  $\hbar\omega / e$  (i.e., equal to the photon energy in electron-Volts). Finally, using Eqs. (7) and (8) we obtain the energy launching efficiency

$$\beta = \frac{\left| \eta_{hi} - \eta_{lo} \right|}{2 + \eta_{hi}\mu_{hi} + \eta_{lo}\mu_{lo}} \quad (14)$$

Note, incidentally, that the top line in Eq. (14) is just the magnitude of the change in transmission  $\Delta T$  between the “low” and “high” states of the modulator. If we are not collecting all the photocurrent or none is generated in the “low” and “high” states, we can proportionately reduce the multiplication factors  $\mu_{lo}$  and  $\mu_{hi}$  respectively (reducing to zero for no photocurrent). For a modulator that does not have photocurrent dissipation (such as a silicon ring or disk [13]) but does nonetheless have only limited change in transmission between the two states, instead of the ideal of  $\beta = 0.5$ , we would therefore have

$$\beta = \Delta T / 2 \quad (15)$$

which we can use for comparison of different kinds of modulators.

We show results for the energy launch efficiency  $\beta$  of various modulators in Table 1. We also give the “energy magnification factor”  $1/\beta$ . The detailed calculations are given in the Appendix.

### 3.6 Example limiting cases

First, we note that a hypothetical modulator with  $\eta_{hi} = 0$ ,  $\eta_{lo} = 1$ , and no additional dissipation from flow of photocurrent in the low state (for example, by having  $V_B = 0$  so that  $\mu_o = 0$ ) would have an energy launching efficiency  $\beta = 0.5$ , as expected for an ideal modulator as discussed above.

To see how this energy efficiency of Eq. (14) behaves more generally, let us presume for simplicity that we are dealing with a high contrast modulator. As mentioned above, with electroabsorption modulators, we need to distinguish between two cases of “normally-on” and “normally-off”.

For a high-contrast modulator in the more common normally-on case, we would have  $\eta_{hi} \approx 1$ , corresponding to essentially no transmission when the “high” voltage is applied. Then

$$\beta \approx \frac{1 - \eta_{lo}}{2 + \mu_{hi} + \eta_{lo}\mu_{lo}} \quad (16)$$

If the modulator was also highly transmitting in its “on” (“low”) bias state, i.e.,  $\eta_{lo} = 0$ , then we obtain the simple formula

$$\beta \approx 1 / (2 + \mu_{hi}) \quad (17)$$

This case is simple to understand physically. In the “high” state, we absorb all of  $E_{ino}$ , and we also have an energy dissipation from photocurrent flow of  $\mu_{hi}E_{ino}$ . In the “low” state, we have  $E_{ino}$  incident energy (which is also transmitted straight through the device). So we have average total input energy  $(1/2)[(E_{ino} + \mu_{hi}E_{ino}) + E_{ino}] = (1/2)E_{ino}(2 + \mu_{hi})$  and average output energy  $E_{ino}/2$ , leading to the ratio Eq. (17)

For the normally-off high contrast case, we would have  $\eta_{lo} \approx 1$ , leading to

$$\beta \approx \frac{1 - \eta_{hi}}{2 + \eta_{hi}\mu_{hi} + \mu_{lo}} \quad (18)$$

If the modulator was also highly transmitting in the “high” state (i.e.,  $\eta_{hi} = 0$ ), then we would have

$$\beta \approx 1 / (2 + \mu_{lo}) \quad (19)$$

### 3.7 Low energy operating modes for electroabsorptive modulators

One interesting possibility for low energy modulator operation is to run the diode into a small forward bias that partially cancels the built-in field of the diode. In quantum well diodes with thin depletion regions (e.g., 150 nm [46]) or very sensitive electroabsorptions (as, for example, in the asymmetric coupled wells of Ref [45].), clear and strong electroabsorption is seen in going from zero bias to small forward bias (0.75 V for Ref [46]. and 1 V for Ref [45].), large enough to make potentially useful modulators.

For example, we could connect the “bottom” terminal of the diode directly to  $V_{DD}$ , eliminating the additional reverse bias supply, equivalently making  $V_B = -V_{DD}$ , as in Fig. 4.

Provided  $V_{DD}$  is significantly smaller in magnitude than the forward turn-on voltage of the diode ( $\sim$ band gap energy of the semiconductor in electron-Volts), the device will still be in small forward bias with small forward current. Obviously, then there is zero total voltage applied across the diode in the “high” state, which makes  $\mu_{hi} = 0$ .  $\mu_{lo}$  actually becomes negative ( $\mu_{lo} = -V_{DD} / (\hbar\omega / e)$ ), so any photocurrent in this state is fed back into the bias supply (or the bypass capacitor  $C_{BP}$  across it). Such a scheme is conceivably viable for Ge quantum well modulators driven from low voltage CMOS. For example, with a  $V_{DD} \sim 0.4\text{V}$ , we could forward bias such a Ge quantum well diode with relatively little forward current. If the depletion region in such a structure was hypothetically  $\sim 80\text{ nm}$  thick, which would allow for several quantum wells, then the built in field in the diode could be  $\sim 8.4 \times 10^4\text{ V/cm}$  with zero bias (presuming a Ge-like diode structure with a band gap energy of  $0.67\text{ eV}$ ), decreasing to  $\sim 3.4 \times 10^4\text{ V/cm}$  with a  $0.4\text{ V}$  forward bias. Such field changes are more than enough for strong electroabsorption with, e.g.,  $10\text{ nm}$  thick Ge wells [23] and for FKE devices.

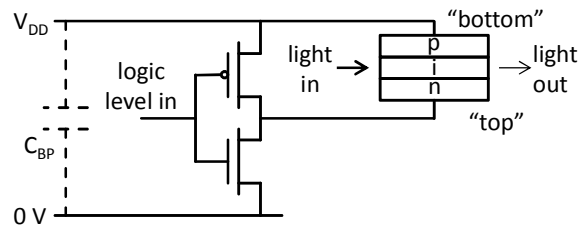


Fig. 4. Example drive circuit for a forward-biased modulator diode.

For a normally-on modulator in the biasing scheme of Fig. 4, there could be some benefit from this photovoltaic forward bias operation in the “low” state, though in a high-contrast modulator in the limit where the modulator is also highly transmitting in the “low” state there would be no actual photocurrent generated in that “low” state because there would be no absorption in that state. The efficiency would then limit to  $\beta = 0.5$  (see Eq. (16) when  $\mu_{hi} = 0$  and  $\eta_{lo} = 1$ ), which is, however, as good as an ideal modulator; here, there would be no excess dissipation from photocurrent flow.

For a normally-off modulator operating at high contrast ( $\eta_{lo} \approx 1$ ) biased as in Fig. 4,

$$\beta \approx (1 - \eta_{hi}) / (2 + \mu_{lo}) \quad (20)$$

For  $\eta_{hi} < -\mu_{lo} / 2$ , where we remember that here  $\mu_{lo} < 0$  in forward bias, the energy launching efficiency  $\beta$  would actually be larger than 50%, better than in an “ideal” modulator. This improvement compared to the “ideal” comes because of the photovoltaic energy generation when the modulator is in its “low” (and strongly absorbing) state.

Whether we run in the normally-on or normally-off modes, driving the modulator into forward bias, especially in the simple biasing scheme of Fig. 4, can lead to very low energy dissipations. In either case, under such biasing we can have situations where there is no energy penalty from the photocurrent generation, with the possibility of even a slight energy benefit from photocurrent in the “normally-off” mode.

#### 4. Total energy dissipation

The core result of this analysis can be summarized in one expression. For a modulator run in reverse bias and/or in a small enough forward bias that any forward current is negligible, or for an insulating modulator, the minimum total (optical plus net electrical) energy required to send a bit of information is on the average

$$E_{bit} = (1/4)CV_{DD}^2 + E_{bit\,trans} / \beta \quad (21)$$

where we presume a driver that is otherwise as efficient as it can be (other than using adiabatic schemes). Here,  $C$  is the modulator capacitance, and  $V_{DD}$  is the peak-to-peak driver voltage (presumed to be the same as the driver supply voltage in calculating dissipated energy).  $E_{bit\,trans}$  is the optical energy or energy difference we want to launch, on average, into the optical channel to send a bit.  $\beta$  is the optical launch efficiency: if the total of all the optical input energy and all the energy dissipated by optical absorption and by photocurrent in the modulator is on the average  $E_{bit\,tot}$  for one bit, then  $\beta = E_{bit\,trans} / E_{bit\,tot}$  (Eq. (7)).  $1/\beta$  can be regarded as an energy magnification factor because it is the number by which the average launched optical energy per bit has to be multiplied when calculating the total energy used by the modulator.

We have established one expression for  $\beta$ , Eq. (14), which works for absorptive modulators, including the effects of absorbed optical power, power dissipation from the flow of photocurrent and even power recovery from photovoltaic effects in forward biased devices. Underlying this expression for  $\beta$  is one formula, Eq. (6), for the static energy (i.e., from absorption and photocurrent) dissipated in the modulator, an expression that holds even for heterojunctions, including quantum wells, and indirect gap semiconductors. If we regard the numerator in Eq. (14) for  $\beta$  more generally as the difference in transmission between the two states of the modulator, and turn off the terms that correspond to power dissipation from photocurrent, the same expression also works for modulators that generate no photocurrent (regardless of whether they are absorptive, refractive, or some combination), in which case the simpler expression Eq. (15) can be used for  $\beta$ . We show example results from published modulators and designs in Table 1.

## 5. Conclusions

Optical modulators are attractive compared to lasers for low-energy dense optical interconnects because they offer threshold-less operation and easier integration with Si. We analyzed energy in modulators that operate in depletion. The analysis applies to diode devices run anywhere from small forward bias (small enough that the forward current is negligible) to large reverse bias, and to insulating modulators. Even with optimally efficient driver circuits, energy consumption occurs from dynamic dissipation in capacitive charging and discharging, from absorbing or otherwise disposing of optical energy that is not transmitted, and any dissipation from flow of photocurrent.

In the dynamic dissipation, we clarified that, provided a bypass capacitor is used on the bias supply, the dynamic energy per bit can indeed be written as  $\Delta E_{bit} = (1/4)CV_{DD}^2$  (Eq. (4)) even though the energy moved in and out of the capacitor can be much larger than this. We also conclude that this dynamic energy is not fundamental. In principle it can be avoided by adiabatic operation, though whether this is practical is still an open question in electronic systems generally.

Our analysis suggests several conclusions for the design of future low-energy modulators. First, reducing the optical energy required at the receiver by, for example, reducing the capacitance of the photodetector and its integration with the transistor circuits helps interconnect links generally to reduce their operating energy per bit. This reduction is, however, particularly important for electroabsorptive modulators because they tend to magnify the energy used through photocurrent dissipation, especially at high bias voltages.

Based on recent results showing low dynamic energies per bit (e.g., 3 fJ/bit [13] and 0.75 fJ/bit [25]), we can conclude that we are going to be able to make modulators with very low dynamic dissipation. Electroabsorption modulators such as those of Ref [25]. could also

exploit resonators to reduce active device length, thereby further reducing capacitance and dynamic dissipation. In electroabsorption devices in particular, photocurrent dissipation will dominate over dynamic dissipation if we run with large bias voltages, however. This suggests we trade off an increase in capacitance for a reduction in voltage, for example employing longer modulators with thinner depletion region (e.g., the designs in Ref [23]).

Use of thin depletion regions in electroabsorption devices could also offer additional energy reductions. For sufficiently thin depletion regions, we could operate with possibly no reverse bias at all, using small forward bias in the “low” state. Such an approach could eliminate photocurrent dissipation entirely. Such designs appear feasible for Ge quantum well QCSE structures, with precedents from previous work in III-V devices [45, 46], as long as diodes with thin intrinsic regions (e.g., ~100 nm or thinner) can be fabricated. In such cases, there is no energy penalty from photocurrent and, because of photovoltaic energy recovery under forward bias, energy efficiencies could equal or even surpass those of hypothetical no-photocurrent devices of the same capacitance, drive voltage and transmission modulation.

### Appendix – Calculation of efficiency factors for Table 1

The GeSi FKE modulator of Ref [14]. runs at 1550 nm ( $\hbar\omega/e \approx 0.8\text{ V}$ ). In our terminology and hypothetically driving with our circuit as in Fig. 2,  $V_{DD} = 3\text{ V}$  and  $V_B = 4\text{ V}$  so  $\mu_{lo} = 4/0.8 \approx 5$  and  $\mu_{hi} = 7/0.8 \approx 8.8$ . Based on a background absorption of  $\sim 2\text{ dB}$  at 0V and their measured modulation depths,  $\eta_{lo} = \eta(4\text{V}) = 0.41$  and  $\eta_{hi} = \eta(7\text{V}) = 0.91$ . From Eq. (14), therefore,  $\beta \approx 4\%$  and  $1/\beta \approx 25$ . Similarly, for the Ge FKE modulator of Ref [15]. running in the middle of their quoted wavelength range at  $\sim 1620\text{ nm}$  ( $\hbar\omega/e \approx 0.77\text{ V}$ ),  $V_{DD} = 4\text{ V}$  and  $V_B = 0\text{ V}$  so  $\mu_{lo} = 0$  and  $\mu_{hi} = 4/0.76 \approx 5.3$ . Again taking numbers in the middle of their quoted ranges gives 2.5 dB loss from absorption in the Ge at 0V and 5.75 dB extinction ratio (and hence a total of 8.25 dB loss from absorption in Ge) at 4V, so we have  $\eta_{lo} \approx 0.44$  and  $\eta_{hi} = 0.85$ , leading to  $\beta \approx 6.3\%$  and  $1/\beta \approx 16$ . For the QCSE modulator of Ref [25]. running at 1460 nm ( $\hbar\omega/e \approx 0.85\text{ V}$ ),  $V_{DD} = 1\text{ V}$  and  $V_B = 4\text{ V}$  so  $\mu_{lo} = 4/0.85 \approx 4.7$  and  $\mu_{hi} = 5/0.85 \approx 5.9$ . The measured extinction ratio of the modulator is  $\sim 3\text{ dB}$ , so  $(1-\eta_{hi})/(1-\eta_{lo}) \approx 0.5$  and from photocurrent measurements,  $\eta_{hi}/\eta_{lo} \approx 2.6$ ; simultaneously solving these two relations gives  $\eta_{hi} \approx 0.62$  and  $\eta_{low} \approx 0.24$ , leading to  $\beta \approx 5.6\%$  and  $1/\beta \approx 18$ . For the proposed QCSE modulator design for 1550 nm ( $\hbar\omega/e \approx 0.8\text{ V}$ ) of Ref [23],  $V_{DD} = 1\text{ V}$  and  $V_B = 0\text{ V}$  so  $\mu_{lo} = 0$  and  $\mu_{hi} = 1/0.8 \approx 1.25$ . For  $\sim 1.4\text{ dB}$  loss at 0 V and  $\sim 6.4\text{ dB}$  loss at 1 V,  $\eta_{lo} \approx 0.27$  and  $\eta_{hi} = 0.77$ , leading to  $\beta \approx 17\%$  and  $1/\beta \approx 6$ . The silicon disk modulator of Ref [13]. has a extinction of 3.8 dB and a loss of  $< 1\text{ dB}$  when used in its low energy 1V drive mode. For a background loss between 0 and 1 dB, these numbers correspond to a  $\Delta T$  of between  $\sim 41\%$  and  $\sim 52\%$  and  $\beta$  (from Eq. (15)) between  $\sim 26\%$  and  $\sim 21\%$ , with corresponding  $1/\beta$  between 4.9 and 3.8.

### Acknowledgments

This work is supported by DARPA UNIC program under Agreement No. HR0011-08-09-0001 between Oracle and the Government, and by the Interconnect Focus Center, one of the six research centers funded under the Focus Center Research Program, a Semiconductor Research Corporation program. DM thanks Ross Audet and Stephanie Claussen for critical readings of the manuscript; all errors remain the responsibility of the author.